1985.

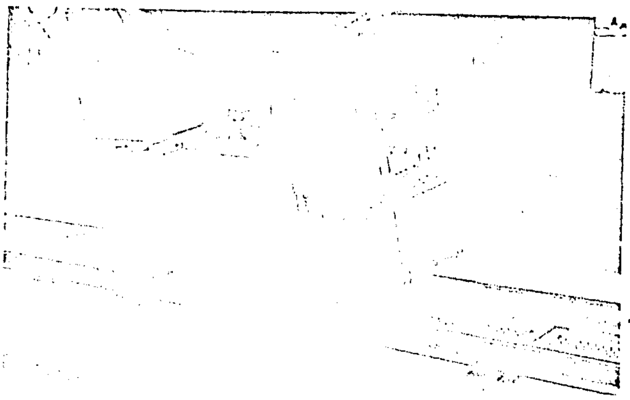

Bild 5: ARAS-Nietautomat für Tonnenmontage

den Anwendungsfall der Spantmontage der Airbus-Schalen ist ein 6-Achsen-NC-Positionierer auf der Basis von Industrierobotern entwickelt. Dieser im kartesischen Koordinatensystem arbeitende Positionierer hat eine Traglast von 100 kg, einen Arbeitsbereich von 10 m × 1,7 m × 3,2 m, die Schwenkachsen sind auf A = ± 45°, B = ± 19°, C = 180° begrenzt und die Masse des fahrenden Ständers beträgt 15 t. Zusätzlich zu der Bahnsteuerung sind 2 Sensoren für die Feinpositionierung installiert. Um die Anlage optimal einsetzen zu können, sind eine automatische Wechselkupplung für den Nietautomaten, Nietbehälter für unterschiedliche Nietlängen, Bohrspäneentsorgung und eine Wartungsbühne mit integriert (Bild 4).

Durch die Entwicklung des rückschlagfreien Niethammers 1980 ist es möglich geworden, damit auch einen Nietautomaten herzustellen, der nicht mehr den Kraftschluß einer Nietquetsche benötigt, sondern durch Hammerschläge (etwa 600/min) den Niet verformt. Dadurch ergab sich der Einsatz, eine Rumpftonne eines Flugzeugs, z.B. des Airbus, auch in dem Bauzustand automatisch zu nieten, der durch die Bauvorrichtung, durch die enormen Abmessungen und die Erfordernis des Kraftschlusses nicht mehr mit quetschenden Nietautomaten möglich ist.

Dieser etwa 100 kg schwere NC-gesteuerte Nietautomat verfährt auf einer Schiene an der Rumpfaußenhaut entlang, bohrt die Nietlöcher, spritzt Dichtmasse in die Senkung, setzt den programmierten Niet aus einem der fünf Nietmagazine ein, kontrolliert das Vorhandensein des Nietes und schlägt den Niet gegen einen ebenfalls rückschlagfreien Gegenhalter. Das Nietschlagen hat jedoch den Nachteil, Lärm zu entwickeln, doch durch Reduzierung der schwingenden Masse und Kapselung der Anlage ist es möglich geworden, den Lärmpegel um 10 dB(A) (gefühlsmäßig die Hälfte) zu senken. Dieses System steht seit Anfang 1984 im Einsatz und wird durch Verbesserung des Gegenhaltersystems für noch flexibleren Einsatz weiterentwickelt (Bild 5).

Zusammenfassung und Ausblick

Mit modernen Nietautomaten ist es gelungen, von kleinsten Baugruppen über großflächige Rumpfschalen zu fertigen Rumpftonnen alle Nietmontagetätigkeiten für Voll-, Blind- und Paßniete mit Hilfe von Nietautomaten auszuführen. Damit wird auch erreicht, daß der Lärmpegel in den Montagehallen auf 85 dB[A) gesenkt wird. Die zukünftige Weiterentwicklung wird durch eine steigende Automatisierung der Bauteilhandhabung und damit Reduzierung der Nebenzeiten der Nietautomaten bestimmt werden. Dazu gehört auch bei kleinen Baugruppen ein rechnergesteuerter Materialfluß, Übergabestationen mit Teileerkennung und Roboter als Positionierer oder als Positioniererbeschicker. Um die Kosten solcher Anlagen in Grenzen zu halten, sind jedoch Richtlinien zu erstellen und vor allem einzubehalten, wie eine automatengerechte Nietbaugruppe konstruiert sein muß.

(Alle Fotos: MBB Bremen)

Autor

Dipl.-Ing. Udo-Henning Stoewer (1942), Stabstelle Fertigungskonzepte und -einrichtungen, MBB Transport- und Verkehrsflugzeuge, Bremen.

J. Kollár, J. Kojnok, L. Kertész, P. Tóth and A. Szász, Budapest

Do dilute aluminium alloys have a heat treatment memory?

(Institute for Solid State Physics, Eötvös University, Budapest)

The heat treatment of aluminium alloys can be performed in different ways. Generally no separate use has been made of the process of heat treatment applied to indicate the state received as the end result only is of importance. The object of the present paper is to examine simple, heat-treated Al-based cable alloys to decide whether the alloy "remembers" how the heat treatment was carried out (in the case of the multistage treatment, what its sequence was). Two extreme types of heat treatment process were applied,namely one using external heat another, using internal heat with direct current. It was taken care that identical alloy states were obtained and the difference of the effect of the two kinds of heat treatment was examined. In doing so, it was looked for a method to deduce a posteriori what kind of heat treatment had been applied previously to the alloy.

Experimental

In the examinations the phase transformations were followed by the differential thermal analysis (DTA) method. The changes sensitive to the method of heat treatment were followed by the usual metallurgical microscopy (LM), by soft X-ray emission spectroscopy (SXES) and, as a control also by X-ray diffraction (XRD).

The substances were simple, very dilute systems (cable materials, composition: Al 99.5%, Fe 0.3 to 0.4%, Si 0.1%). These models were subjected to different heat treatments, namely external heating by the normal furnace, by applying a flame, and by the plasma type treatment. Also an internal ohmic heating by direct current was performed. To clarify the memory effects, the changes of the surface oxide layer were also examined by investigating separately their chemical bond states. The heat treatments were performed within conditions of external solution heat treatment, while the intensity of the internal heating was regulated by controlling the current density.

Results

The examined samples were in identical physical state as evidenced by DTA, but were heat treated in different manners. The dissimilarities in the heat effect changed essentially two parameters:

1. The morphological, grain-structure properties,
2. The properties of the covering oxide layer.

The type 1 changes were studied by examining metallographically the appropriate, polished metal samples while the type 2 changes, were examined by SXES and XRD to determine the structure, the thickness and the chemical bond states in the oxide layer. As a result of a short-time (min. 5 s), direct current of a (10^7 A/m²) current density recrystallization cannot be seen. At the same time, there is a limit of current density ($6 \cdot 10^7$ A/m²) which causes no visible recrystallization within 6 s. After 8 s, however, the system swings over suddenly and polyhedral grains can be seen. This phenomenon is more pronounced at higher current density and in the case of a current density of 10^8 A/m², the sample seems to explode after 6 s. As to the behaviour in time, also at low current density (at $2 \cdot 10^7$ A/m²) one can see already after 15 s the "thickening" of the deformed grains reflecting the direction of the drawing which, after 30 s, is quite apparent. The recrystallization is already complete within 40 s. This is already complete in 9 s at a current density of $5 \cdot 10^8$ A/m².

Simultaneously the type of recrystallization under the effect of the isothermal heat treatment at 300°C shows unambiguously that the heat treatment had been an external one, as opposed to the previous case applying a direct current (see fig. 1).

The soft X-ray emission examinations were conducted to examine the "memory effect" of the oxide layer. On the basis of the examination of the Al K_α and O K_α spectra we can summarize our conclusions as follows:

At the beginning, on the wires without any treatment, there is an Al_2O_3 layer 5 nm thick.

As a result of external heating by plasma (spark)-process, an oxide layer 40 to 50 nm thick is formed which is analogous chemically with the former one.

If the layer is heated further in a flame at 600°C, it undergoes a chemical transformation and the thickness increases further by 5 to 10 nm.

Also, simple flaming (without sparks) results in the thickening of the oxide layer but to a much lesser extent (10 to 20 nm) and this oxide differs from each of the former ones.

a/b

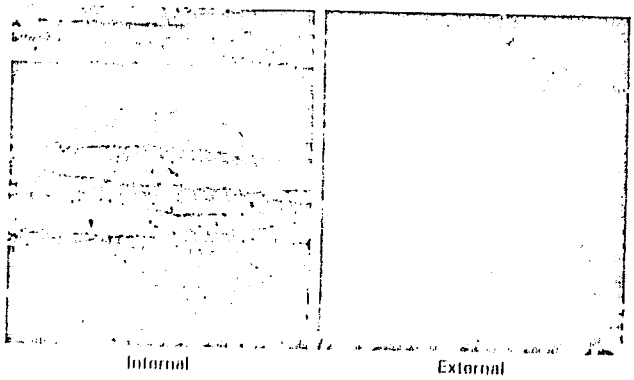

Figs. 1a and b: The morphology of the internally (fig. 1a) and externally (fig. 1b) heat treated alloys; ×45

The determining of the exact $O_{K_\alpha}/Al_{K_\alpha}$ ratio makes it even possible to estimate the DC-plasma current. Some SXE spectra are shown in fig. 2.

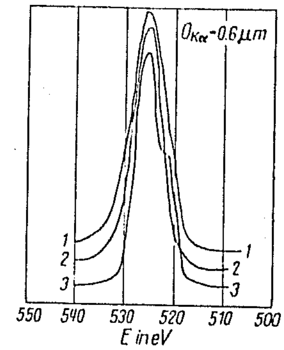

Fig. 2: Some SXES spectra for investigation of aluminium-oxide layers; 1 not heat treated, 2 simple flaming, 3 flaming and sparking ($J = 1 \cdot 10^8$ A/m²)

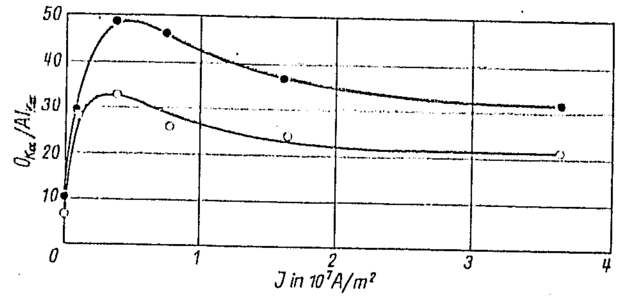

Fig. 3: The current-density dependence of the SXES intensity ratio for O K_α and Al K_α lines originating from a depth of 0.2 µm from the surface; ● external heat treatment, O internal heat treatment

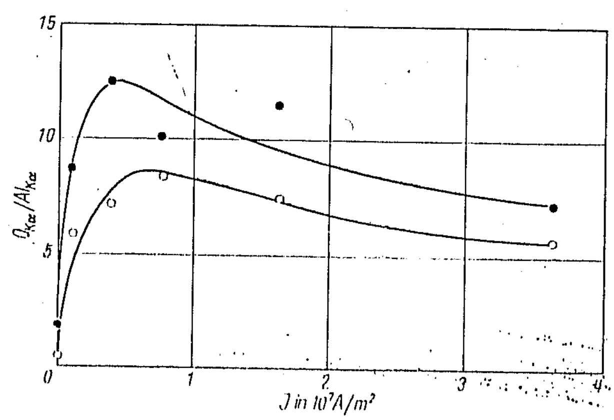

Fig. 4: The current-density dependence of the SXES intensity ratio for O K_α and Al K_α lines, originating from a depth of 0.6 µm from the surface; ● external heat treatment, O internal heat treatment

Conclusion

In the alloy states the specific effect of the heat treatment processes can be definitely demonstrated. The memory effect of the alloy and surface states can be observed and subsequently used to trace back the type of the previous heat treatment; moreover, in the case of the use of a set of heat treatments, their sequence can also be traced. It can be shown that the behaviour of the oxide layer, in addition to the preceding information, carries also the characteristics of the heat treating DC-plasma current density which can also be determined by a simple intensity relationship (see figs. 3 and 4).

Authors

József Kollár (1945), Assistant, Lecturer,

József Kojnok, Dr. (1954), As. Lecturer,

László Kertész, Ao. Prof. (1926), Head of Department,

Péter Tóth (1954), Assistant,

András Szász, Dr., Ao. Prof. (1947), Head of Laboratory,

all: Institute for Solid State Physics, Eötvös University, Budapest (Hungary).